

On the Numerical Treatment of the Time-Dependent Schrödinger Equation in Two Dimensions

Simon Wenchel and Lasse Kreimendahl

July 29, 2025

Contents

1	Introduction	2
2	Finite Element Method	4
3	Physics-Informed Neural Networks	10
4	Experiments and Discussion	12
5	Outlook	21

1 Introduction

The time-dependent Schrödinger equation lies at the heart of quantum mechanics, dictating how the state of a quantum system evolves under the influence of potential energy landscapes. In contrast to classical mechanics, which predicts trajectories, the Schrödinger equation predicts wave functions, whose squared modulus yields probability densities. This shift from deterministic paths to probabilistic amplitudes marks a fundamental departure from classical intuition.

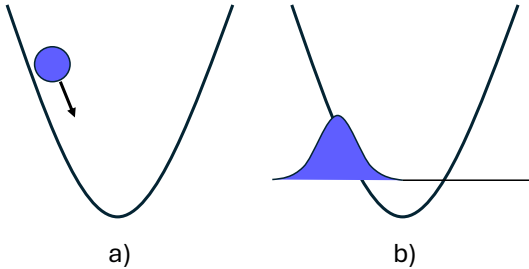


Figure 1: Illustration of the principles of classical and quantum mechanics. a) In classical mechanics, the state of a system is described by a point in phase space, which evolves deterministically according to the laws of motion. b) In quantum mechanics, the state of a system is described by a wave function, which encodes the probability of finding the system in a given state.

From fundamental atomic models to emergent quantum technologies, the ability to solve the Schrödinger equation accurately and efficiently is essential for predicting quantum behavior. Yet, in most realistic settings, analytic solutions are unavailable. This necessitates the development of robust numerical approaches.

In molecular systems, the Schrödinger equation governs the motion of nuclei on potential energy surfaces obtained from electronic structure calculations. Within the Born-Oppenheimer approximation, these nuclei behave as quantum particles subject to high-dimensional, often complex potentials. For example, when modeling the movement of atoms within a molecule, it is common to reduce the full-dimensional problem to a few key internal coordinates, such as bond stretching or rotations. Even in such simplified spaces, the time evolution of a quantum state can reveal complex phenomena such as tunneling (where a particle passes through a potential barrier it classically could not cross), interference (where overlapping wave functions amplify or cancel each other), or wave packet spreading (the dispersion of a localized quantum state over time)—none of which are accessible through classical approximations.

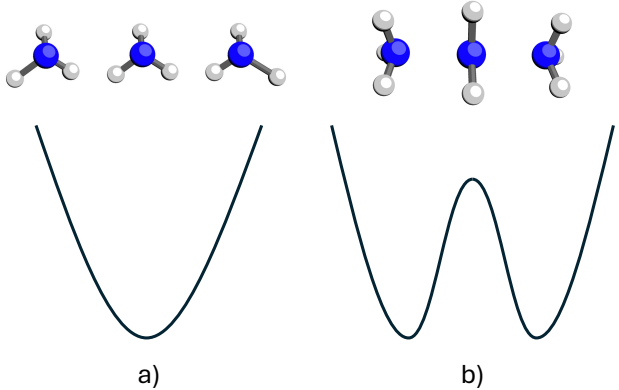


Figure 2: Example of a potential energy surface for a molecule (ammonia), where the nuclei are described by a few key internal coordinates. a) For bond stretching, this energy surface can be approximated by a harmonic potential. b) For some more complex motions, the potential energy surface can be approximated by a double well potential.

This report investigates the numerical solution of the time-dependent Schrödinger equation in two spatial dimensions, a setting that permits the exploration of realistic molecular scenarios while maintaining computational tractability. Specifically, we consider model systems where the potential energy surface encodes features representative of atomic motions, reactive pathways, or coupled physical effects.

To address this problem, we compare two distinct numerical strategies. The first is the finite element method (FEM), a classical and rigorously grounded approach based on variational formulations. The second leverages recent advances in machine learning: physics-informed neural networks (PINNs), which approximate the solution by minimizing the residual of the governing equations within a data-driven framework. While FEM offers precision and theoretical guarantees, PINNs provide flexibility and mesh-free generalization—particularly attractive for high-dimensional or inverse problems.

Through this dual lens, the report aims to highlight both the challenges and opportunities inherent in solving quantum dynamical equations numerically, and to evaluate the strengths of different computational paradigms in a physically meaningful context.

2 Finite Element Method

Model Problem: Schrödinger Equation

The Schrödinger equation is a second-order partial differential equation that describes the time evolution of a quantum system, represented by its wave function.

Let $\Omega \subset \mathbb{R}^n$ be a bounded Lipschitz domain and let $V : \Omega \times [0, T] \rightarrow \mathbb{R}$ be a given potential. We say that a function

$$u : \Omega \times [0, T] \rightarrow \mathbb{C}$$

is a **solution to the time-dependent Schrödinger equation, with homogeneous Dirichlet boundary conditions** if it satisfies the following system of equations:

$$\begin{aligned} i\partial_t u(x, t) &= -\Delta u(x, t) + V(x, t)u(x, t), \quad x \in \Omega, \quad t > 0, \\ \partial_t u(x, 0) &= u_0(x), \quad x \in \Omega, \\ u(x, t) &= 0, \quad x \in \partial\Omega, \quad t > 0, \end{aligned}$$

where Δ is the Laplacian operator, $V(x, t)$ is a potential, $\partial\Omega$ is the boundary of the domain Ω , and $u_0(x)$ is the initial condition at time $t = 0$.

The function $u(x, t)$ represents the wave function of the quantum system at position x and time t . The term $i\partial_t u(x, t)$ represents the time evolution of the wave function, while the term $-\Delta u(x, t)$ accounts for the kinetic energy of the system. The potential term $V(x, t)u(x, t)$ describes the interaction of the wave function with an external potential.

Weak Formulation of Schrödinger's Equation

To derive the weak formulation of the time dependent Schrödinger equation, we multiply the equation by \bar{v} , the complex conjugate of the test function $v(x, t) \in H_0^1(\Omega; \mathbb{C})$ and integrate over the domain Ω .

Sobolev Space with Complex Values Let $\Omega \subset \mathbb{R}^d$ be a bounded Lipschitz domain. We define the complex Sobolev space

$$H_0^1(\Omega; \mathbb{C}) := \{u \in L^2(\Omega; \mathbb{C}) \mid \nabla u \in L^2(\Omega; \mathbb{C}^d), u|_{\partial\Omega} = 0\}.$$

This space is equipped with the inner product

$$\langle u, v \rangle_{H_0^1(\Omega)} := \int_{\Omega} \nabla u \cdot \nabla \bar{v} \, dx + \int_{\Omega} u \bar{v} \, dx,$$

and the associated norm

$$\|u\|_{H_0^1} := \sqrt{\langle u, u \rangle_{H_0^1}}.$$

By utilizing Greens' identity, we can transform the second order differential equation into a first order weak formulation:

$$\begin{aligned} \int_{\Omega} \Delta u \bar{v} dx &= \int_{\Omega} \nabla u \cdot \nabla \bar{v} dx - \int_{\partial\Omega} \nabla u \cdot n \bar{v} ds, \\ &= \int_{\Omega} \nabla u \cdot \nabla \bar{v} dx, \quad (\text{since } u \text{ vanishes on } \partial\Omega). \end{aligned}$$

This leads to the weak formulation of the Schrödinger equation:

$$i \int_{\Omega} (\partial_t u) \bar{v} dx = - \int_{\Omega} \nabla u \cdot \nabla \bar{v} dx + \int_{\Omega} V(x, t) u \bar{v} dx.$$

We take the complex conjugate of the test function v to ensure that the formulation aligns with the sesquilinear inner product in Hilbert spaces like $L^2(\Omega; \mathbb{C})$ and $H_0^1(\Omega; \mathbb{C})$.

Time Integration with the Euler Method

The Euler method is a simple and widely used numerical method for solving differential equations. It approximates the time derivative with a first order finite difference scheme. In the following we will use the Backward Euler method, which gives an approximation of the time derivative as follows:

$$\partial_t u(x, t) \approx \frac{u^{t+dt} - u^t}{dt},$$

The Backward Euler method allows us to solve the Schrödinger equation iteratively in each time step by finite elements method in space. The time resolution is controlled by the time step size dt , where t is the current time and $t + dt$ is the next time step.

The Backward Euler method has a remaining error of order $\mathcal{O}(dt)$, which means that the error decreases linearly with the time step size. This is sufficient for many applications, but for higher accuracy, higher order methods such as the Crank-Nicolson method or Runge-Kutta methods can be used.

Weak Formulation with Backward Euler Method

The time-discrete weak form of the Schrödinger equation becomes:

$$i \int_{\Omega} \left(\frac{u^{t+dt} - u^t}{dt} \right) \bar{v} dx = - \int_{\Omega} \nabla u^{t+dt} \cdot \nabla \bar{v} dx + \int_{\Omega} V(x, t) u^{t+dt} \bar{v} dx$$

By rearranging, the weak formulation takes the form, with implicit terms on the left and explicit (known) terms on the right:

$$i \int_{\Omega} u^{t+\text{dt}} \bar{v} - \text{dt} \int_{\Omega} u^{t+\text{dt}} \bar{v} V(x, t) dx + \text{dt} \int_{\Omega} \nabla u^{t+\text{dt}} \cdot \nabla \bar{v} = i \int_{\Omega} u^t \bar{v} dx,$$

$$a(u^{t+\text{dt}}, v) = L(v),$$

which can be solved iteratively for $u^{t+\text{dt}}$ in each time step.

Existence and Uniqueness via the Lax-Milgram Theorem in Complex Hilbert Spaces

To establish the existence and uniqueness of solutions to the weak formulation of the Schrödinger equation, we can apply the Lax-Milgram theorem. This theorem provides conditions under which a sesquilinear form defines a unique solution to a linear functional equation in a Hilbert space.

Theorem 2.1 (Lax-Milgram Theorem). *Let H be a complex Hilbert space with inner product $\langle \cdot, \cdot \rangle$ and norm $\|\cdot\|_H$. Let $a : H \times H \rightarrow \mathbb{C}$ be a sesquilinear form, i.e.,*

$a(\cdot, v)$ is linear for all $v \in H$, $a(u, \cdot)$ is conjugate-linear for all $u \in H$.

Suppose that:

1. **Boundedness of the sesquilinear form:** *There exists $M > 0$ such that*

$$|a(u, v)| \leq M \|u\|_H \|v\|_H \quad \text{for all } u, v \in H.$$

2. **Boundedness of the linear form:** *There exists $C > 0$ such that*

$$|L(v)| \leq C \|v\|_H \quad \text{for all } v \in H.$$

3. **Coercivity:** *There exists $\alpha > 0$ such that*

$$\Re a(u, u) \geq \alpha \|u\|_H^2 \quad \text{for all } u \in H.$$

Then for every bounded linear functional $L \in H^$, there exists a unique $u \in H$ such that*

$$a(u, v) = L(v) \quad \text{for all } v \in H.$$

Application of the Lax-Milgram Theorem to the Discrete Schrödinger Equation

In the following, we will show the conditions of the Lax-Milgram theorem are satisfied for the sesquilinear form $a(u, v)$ and the linear functional $L(v)$, such that the existence and uniqueness of the solution to the weak formulation of the Schrödinger equation are guaranteed.

As we have already established, the Sobolev space $H_0^1(\Omega; \mathbb{C})$ is a Hilbert space with the inner product:

$$\langle u, v \rangle_{H_0^1(\Omega)} := \int_{\Omega} \nabla u \cdot \nabla \bar{v} dx + \int_{\Omega} u \bar{v} dx.$$

Boundedness of the Sesquilinear and Linear Form.

Lemma 2.2 (Boundedness of $a(u, v)$). *Let $u, v \in H_0^1(\Omega; \mathbb{C})$, $V \in L^\infty(\Omega)$ and $\tau > 0$. Then the sesquilinear form $a(u, v)$ is bounded, i.e., there exists $M > 0$ such that*

$$|a(u, v)| \leq M \|u\|_{H_0^1} \|v\|_{H_0^1}.$$

Proof. By triangle inequality, we can split the sesquilinear form into three terms:

$$|a(u, v)| \leq \left| \int_{\Omega} \nabla u \cdot \nabla \bar{v} dx \right| + \left| \frac{i}{dt} \int_{\Omega} u \bar{v} dx \right| + \left| \int_{\Omega} V(x, t) u^{t+dt} \bar{v} dx \right|.$$

We estimate each term separately.

(1) Stiffness term:

$$\begin{aligned} \left| \int_{\Omega} \nabla u \cdot \nabla \bar{v} dx \right| &\leq \int_{\Omega} |\nabla u| |\nabla \bar{v}| dx = \int_{\Omega} |\nabla u| |\nabla v| dx \\ &\leq \|\nabla u\|_{L^2(\Omega)} \|\nabla v\|_{L^2(\Omega)} \quad (\text{by Cauchy-Schwarz in } L^2(\Omega; \mathbb{C}^d)). \end{aligned}$$

(2) Mass term:

$$\begin{aligned} \left| \int_{\Omega} \frac{i}{dt} u \bar{v} dx \right| &= \frac{1}{dt} \left| \int_{\Omega} u \bar{v} dx \right| \leq \frac{1}{dt} \int_{\Omega} |u| |v| dx \\ &\leq \frac{1}{dt} \|u\|_{L^2(\Omega)} \|v\|_{L^2(\Omega)} \quad (\text{again by Cauchy-Schwarz}). \end{aligned}$$

(3) Potential term:

$$\begin{aligned} \left| \int_{\Omega} V(x, t) u^{t+dt} \bar{v} dx \right| &\leq \|V\|_{L^\infty(\Omega)} \int_{\Omega} |u^{t+dt}| |\bar{v}| dx \\ &\leq \|V\|_{L^\infty(\Omega)} \|u^{t+dt}\|_{L^2(\Omega)} \|v\|_{L^2(\Omega)}. \end{aligned}$$

Combining all terms:

$$\begin{aligned} |a(u, v)| &\leq \|\nabla u\|_{L^2} \|\nabla v\|_{L^2} + \frac{1}{dt} \|u\|_{L^2} \|v\|_{L^2} + \|V\|_{L^\infty} \|u^{t+dt}\|_{L^2} \|v\|_{L^2} \\ &\leq M (\|\nabla u\|_{L^2} \|\nabla v\|_{L^2} + \|u\|_{L^2} \|v\|_{L^2}), \\ &\leq M \|u\|_{H_0^1} \|v\|_{H_0^1}, \quad (\text{by Cauchy-Schwarz}) \end{aligned}$$

where $M = \max(1, \frac{1}{dt} + \|V\|_{L^\infty})$. ■

Lemma 2.3 (Boundedness of the linear form). *Let $u^t \in L^2(\Omega; \mathbb{C})$ be given. Then the linear functional*

$$L(v) := \frac{i}{dt} \int_{\Omega} u^t \bar{v} dx$$

is bounded on $H_0^1(\Omega; \mathbb{C})$. That is, there exists a constant $C > 0$ such that

$$|L(v)| \leq C \|v\|_{H_0^1(\Omega)} \quad \forall v \in H_0^1(\Omega; \mathbb{C}).$$

Proof. We estimate each term separately using the Cauchy-Schwarz and Hölder inequalities.

$$\begin{aligned} |L(v)| &\leq \left| \frac{i}{dt} \int_{\Omega} u^t(x) \bar{v}(x) dx \right| = \frac{1}{dt} \left| \int_{\Omega} u^t(x) \bar{v}(x) dx \right| \\ &\leq \frac{1}{dt} \int_{\Omega} |u^t(x)| |v(x)| dx \quad (\text{by triangle inequality}) \\ &\leq \frac{1}{dt} \|u^t\|_{L^2(\Omega)} \|v\|_{L^2(\Omega)} \quad (\text{by Cauchy-Schwarz inequality}). \end{aligned}$$

As in the last proof we can split $\|v\|_{L^2(\Omega)} = \frac{1}{2} \|v\|_{L^2(\Omega)}^2 + \frac{1}{2} \|v\|_{L^2(\Omega)}^2$ and use the Poincaré inequality which gives us:

$$|L(v)| \leq \frac{\tilde{C}}{2} \left(\|\nabla v\|_{L^2(\Omega)}^2 + \|v\|_{L^2(\Omega)}^2 \right) \leq C \|v\|_{H_0^1(\Omega)}^2,$$

where $C = \frac{1}{2dt} \|u^t\|_{L^2(\Omega)}$. ■

Hence, L is bounded. ■

Coercivity of the Sesquilinear Form

Lemma 2.4 (Coercivity of the sesquilinear form). *Let $a(u, v)$ be the sesquilinear form defined by*

$$a(u, v) = \int_{\Omega} \nabla u \cdot \nabla \bar{v} dx + \frac{i}{dt} \int_{\Omega} u \bar{v} dx - \int_{\Omega} V(x, t) u \bar{v} dx.$$

Then there exists a constant $\alpha > 0$ such that

$$\Re a(u, u) \geq \alpha \|u\|_{H_0^1(\Omega)}^2 \quad \forall u \in H_0^1(\Omega; \mathbb{C}).$$

Proof. We compute the real part of $a(u, u)$: Note: check again for minus signs looks weird

$$\begin{aligned} \Re a(u, u) &= \Re \left(\int_{\Omega} |\nabla u|^2 dx + \frac{i}{dt} \int_{\Omega} |u|^2 dx - \int_{\Omega} V(x, t) u \bar{u} dx \right) \\ &= \int_{\Omega} |\nabla u|^2 dx - \int_{\Omega} V(x, t) |u|^2 dx \\ &= \|\nabla u\|_{L^2(\Omega)}^2 - \|V\|_{L^\infty(\Omega)} \|u\|_{L^2(\Omega)}^2. \end{aligned}$$

By the boundedness of the potential term, we have:

$$\|V\|_{L^\infty(\Omega)} = C_V < \infty$$

By the Poincaré inequality, we have:

$$\|u\|_{L^2(\Omega)}^2 \leq C_P \|\nabla u\|_{L^2(\Omega)}^2 \quad (\text{for some constant } C_P > 0).$$

Thus, we can estimate for $\Re a(u, u)$:

$$\begin{aligned} \Re a(u, u) &= \|\nabla u\|_{L^2(\Omega)}^2 - C_V \|u\|_{L^2(\Omega)}^2 \\ &\geq \|\nabla u\|_{L^2(\Omega)}^2 - C_V C_P \|\nabla u\|_{L^2(\Omega)}^2 \\ &= (1 - C_V C_P) \|\nabla u\|_{L^2(\Omega)}^2. \end{aligned}$$

By definition of the H_0^1 norm and Poincaré inequality, we have:

$$\|u\|_{H_0^1(\Omega)}^2 = \|\nabla u\|_{L^2(\Omega)}^2 + \|u\|_{L^2(\Omega)}^2 \leq (1 + C_P) \|\nabla u\|_{L^2(\Omega)}^2.$$

and therefore:

$$\|u\|_{L^2(\Omega)}^2 \geq \frac{1}{1 + C_P} \|\nabla u\|_{H_0^1(\Omega)}^2.$$

Combining these estimates, we obtain:

$$\begin{aligned} \Re a(u, u) &\geq (1 - C_V C_P) \|\nabla u\|_{L^2(\Omega)}^2 \\ &\geq \frac{1 - C_V C_P}{1 + C_P} \|u\|_{H_0^1(\Omega)}^2. \end{aligned}$$

Thus, we can choose $\alpha = \frac{(1 - C_V C_P)}{(1 + C_P)} > 0$ if $C_V < 1/C_P$ and the real part of the sesquilinear form is coercive.

■

We showed that every condition of the Lax-Milgram theorem is satisfied, thus a solution to the weak formulation of the Schrödinger equation exists and is unique.

3 Physics-Informed Neural Networks

Physics-Informed Neural Networks (PINNs) can be used to solve the Schrödinger equation by incorporating the physics of the problem into the training process. The neural network is trained to minimize a loss function that includes terms for the residual of the Schrödinger equation, initial conditions, and boundary conditions.

Classical PINN Loss for the Schrödinger Equation

Let $u_\theta : \Omega \times [0, T] \rightarrow \mathbb{R}^2$ be a neural network approximation to the solution of the time-dependent Schrödinger equation

$$i \partial_t u = -\Delta u + V(x, t)u.$$

The output of the neural network is a two dimensional real vector, representing the real and imaginary parts of the wave function u . To train the neural network, we define a loss functional that combines the residual of the Schrödinger equation, initial conditions, boundary conditions and a normalization term.

Residual Loss The residual function origins directly from the Schrödinger equation and measures how well the neural network satisfies the PDE at given collocation points in space and time. We define the residual function

$$\mathcal{R}(x, t) := i \partial_t u_\theta(x, t) + \Delta u_\theta(x, t) - V(x, t)u_\theta(x, t).$$

If the Residual function is zero, the neural network satisfies the Schrödinger equation at the collocation point (x, t) . And therefore the residual functional is defined as

$$\mathcal{L}_{\text{PDE}}(\theta) = \frac{1}{N_R} \sum_{j=1}^{N_R} |\mathcal{R}(x_j, t_j)|^2,$$

where N_R is the number of collocation points, and $(x_j, t_j) \in \Omega \times (0, T]$.

Initial Condition Loss To enforce the initial condition $u(x, 0) = u_0(x)$, we define the initial condition loss as

$$\mathcal{L}_{\text{IC}}(\theta) = \frac{1}{N_0} \sum_{j=1}^{N_0} |u_\theta(x_j, 0) - u_0(x_j)|^2,$$

where $u_0(x)$ is the given initial condition and $(x_j, 0) \in \Omega \times \{0\}$ and N_0 is the number of collocation points.

Boundary Condition Loss The boundary condition is enforced by minimizing:

$$\mathcal{L}_{\text{BC}}(\theta) = \frac{1}{N_B} \sum_{j=1}^{N_B} |u_\theta(x_j, t_j) - 0|^2,$$

where $(x_j, t_j) \in \partial\Omega \times (0, T]$ and N_B is the number of collocation points on the boundary.

Normalization Loss To ensure the neural network does not converge to the trivial solution $u(x, t) = 0$, we can add a normalization term to the loss function. This term can be defined as:

$$\mathcal{L}_{\text{norm}}(\theta) = \left(C - \frac{1}{N_N} \sum_{j=1}^{N_N} |u_\theta(x_j, t_j)|^2 \right)^2,$$

where $(x_j, t_j) \in \Omega \times (0, T]$ and N_N is the number of collocation points. This describes the difference of the L^2 norm of the neural network output to a constant value C .

Total Loss Functional The total loss functional combines all the individual losses with weighting parameters:

$$\mathcal{L}_{\text{PINN}}(\theta) = \lambda_{\text{PDE}} \cdot \mathcal{L}_{\text{PDE}}(\theta) + \lambda_{\text{IC}} \cdot \mathcal{L}_{\text{IC}}(\theta) + \lambda_{\text{BC}} \cdot \mathcal{L}_{\text{BC}}(\theta) + \lambda_{\text{norm}} \cdot \mathcal{L}_{\text{norm}}(\theta).$$

Minimizing this loss functional with respect to the neural network parameters θ will yield a solution that approximates the Schrödinger equation while satisfying the initial and boundary conditions.

4 Experiments and Discussion

To compare the performance of the FEM and PINNs, we consider the following two problems:

Problem 1: Free Schrödinger Equation on the Unit Square

We consider the time-dependent Schrödinger equation on the unit square $\Omega = (0, 1)^2$ with homogeneous Dirichlet boundary conditions and zero potential over the time interval $[0, 1]$:

$$\begin{aligned} i \partial_t u(x, t) &= -\Delta u(x, t), && \text{in } \Omega \times (0, T), \\ u(x, t) &= 0, && \text{on } \partial\Omega \times (0, T), \\ u(x, 0) &= u_0(x), && \text{in } \Omega. \end{aligned}$$

A known exact solution is given by the separable function

$$u(x, t) = \sin(\pi x_1) \sin(\pi x_2) e^{-i2\pi^2 t},$$

which satisfies:

- The homogeneous Dirichlet boundary conditions: $u(x, t) = 0$ on $\partial\Omega$ for all t ,
- The initial condition: $u_0(x) = \sin(\pi x_1) \sin(\pi x_2)$,
- The PDE:

$$\Delta u = -2\pi^2 \sin(\pi x_1) \sin(\pi x_2) e^{-i2\pi^2 t}, \quad \partial_t u = -i2\pi^2 \sin(\pi x_1) \sin(\pi x_2) e^{-i2\pi^2 t},$$

hence

$$i \partial_t u = -\Delta u.$$

The analytical solution at time $t = 0$ is shown in Figure 3. Note that in the following, we will always show $|u(x, t)|^2$, as this is the physically relevant quantity.

FEM Solution

We use the variational formulation of the Schrödinger equation derived above, by setting $V(x, t) = 0$ we obtain the weak formulation of the free Schrödinger equation.

We summarize the parameters of the problem as follows:

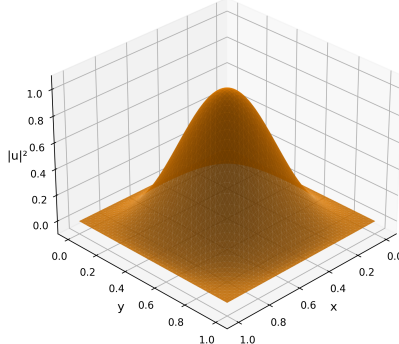


Figure 3: Analytical solution at time $t = 0$ of the free Schrödinger equation on the unit square.

- Meshing: Triangular mesh with 64×64 elements
- Elements: P1 Lagrange elements
- Time step size: $\Delta t = 0.00001$

The evolution of the solution for different time steps is shown in Figure 4.

We can see that the square of the absolute value of the wave function is constant over time, which is expected from the analytical solution.

Error Analysis

The approximation error of the numerical solution has two components:

- the discretization error due to the finite element method,
- the time-stepping error due to the Backward Euler method.

We define the error vector $e_h^{(t)}$ as the difference between the numerical solution $u_h^{(t)}$ and the exact solution $u^{(t)}$ at each time step:

$$e_h^{(t)} = u_h^{(t)} - u^{(t)}.$$

Figure 5 shows the L^2 norm of the error vector over time for different mesh sizes. From this plot we can see that the error increases linearly with time, which is

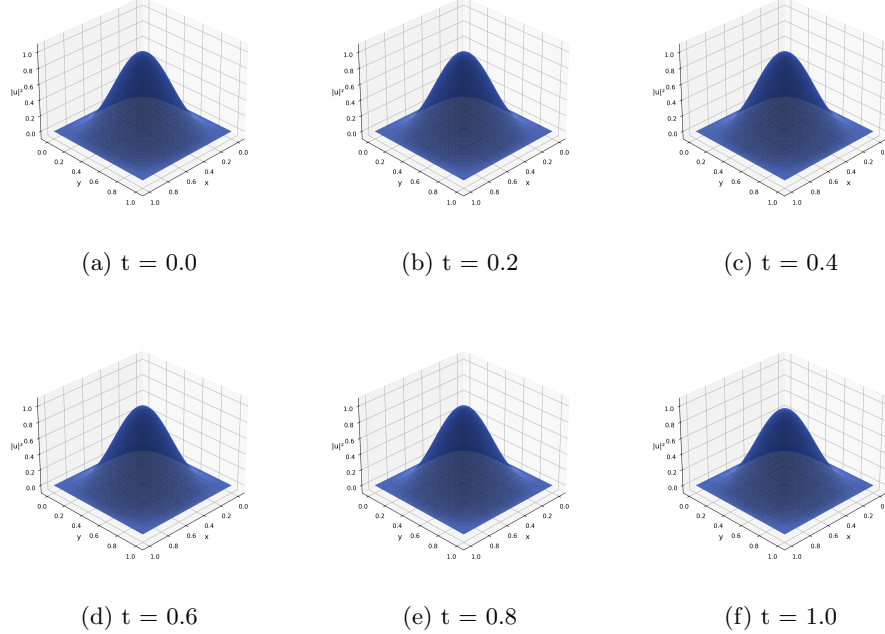


Figure 4: Time evolution of the solution of the free Schrödinger equation, obtained with the FEM.

expected for the Backward Euler method. For finer meshes the absolute error is smaller, as the FEM discretization error decreases, but the time error remains. This becomes particularly evident for the refinements $n = 64, 128, 256$ where the error behaves almost the same for all resolutions.

Figure 6 shows the L^2 norm of the error vector over mesh sizes for different timesteps. It also shows a reference line described of order $\mathcal{O}(h^2)$, which is the expected convergence rate for the FEM with P1 elements. We see that for coarser meshes the error perfectly meets the slope of the reference line. Again for the last three refinements $h = 1/64, 1/128, 1/256$ the error does not decrease significantly anymore, which indicates again, that the time stepping error dominates the overall error. It also gets obvious that through error propagation the error increases with time, which is expected for the Backward Euler method.

PINN Solution

We use the previously derived PINN loss functional to train a neural network to approximate the solution of the free Schrödinger equation, by setting the potential $V(x, t) = 0$ and the initial condition $u_0(x) = \sin(\pi x_1) \sin(\pi x_2)$.

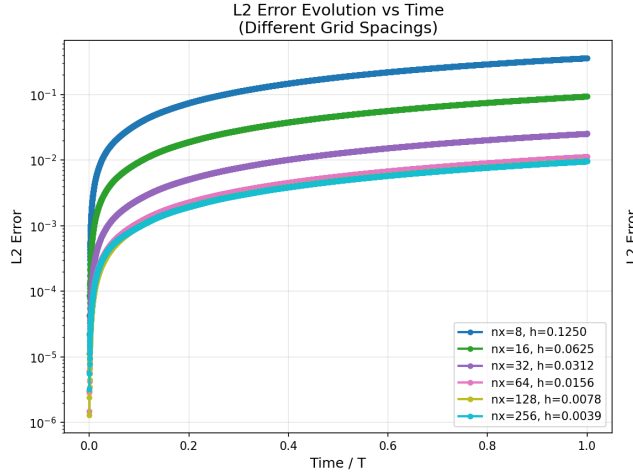


Figure 5: Error analysis for the FEM solution of the free Schrödinger equation on the unit square. The error increases linearly with time, which is expected for the Backward Euler method. For finer meshes the absolute error is smaller, as the FEM discretization error decreases, but the time error remains.

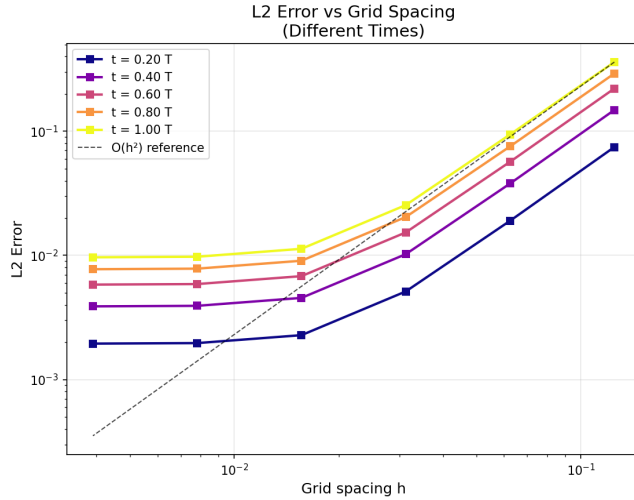


Figure 6: Error analysis for the FEM solution of the free Schrödinger equation on the unit square. The error as a function of the mesh size is on the order of $\mathcal{O}(h^2)$, which is the expected convergence rate for the FEM with P1 elements. Only for very fine grids, the error is dominated by the time stepping error.

Through a hyperparameter optimization we found the following parameters to work well:

- Hidden layers: 3
- Neurons per layer: 128
- Activation function: Tanh
- Learning rate: 0.00003
- Interior collocation points: 50000
- Boundary and initial collocation points: 25000 each
- $\lambda_{\text{PDE}} = 1.0$, $\lambda_{\text{IC}} = 1.0$, $\lambda_{\text{BC}} = 1.0$, $\lambda_{\text{norm}} = 0$

The evolution of the model prediction computed by the PINN is shown in Figure 7. We can see that the PINN is able to approximate the initial and boundary condition well, but does not show the constant behavior of the analytical solution over time. Instead, the solution converges to the trivial solution $u(x, t) = 0$ over time, which formally satisfies the PDE and boundary conditions but is physically uninformative. This behavior could not be resolved by adding the normalization term to the loss functional, which was intended to prevent the trivial solution. Note that at least in theory, $\|u(x, t)\|^2 = 1$ must hold for all t , as the probability of finding a particle in the domain must be 1.

Comparison of FEM and PINN

Finite Element Methods have the advantage of a well-established theory with which the convergence and stability of the solution can be guaranteed. Furthermore, the desired accuracy can be achieved by refining the mesh and the time step size. This is in stark contrast to PINNs, where many different hyperparameters have a strong influence on the solution and therefore the accuracy. In this particular case, the PINN is not capable of approximating the analytical solution, which is a major drawback. We aim to resolve this problem to have the ability to compare the solutions of both methods.

Problem 2: Schrödinger Equation with Time-Dependent Model Potential

In addition to the free Schrödinger equation, we will now consider a non-zero potential. Since we want to model the time evolution of the wave function, we are particularly interested in potentials that have an explicit time dependence:

$$V(x, t) = V_0(x) + V'(x, t),$$

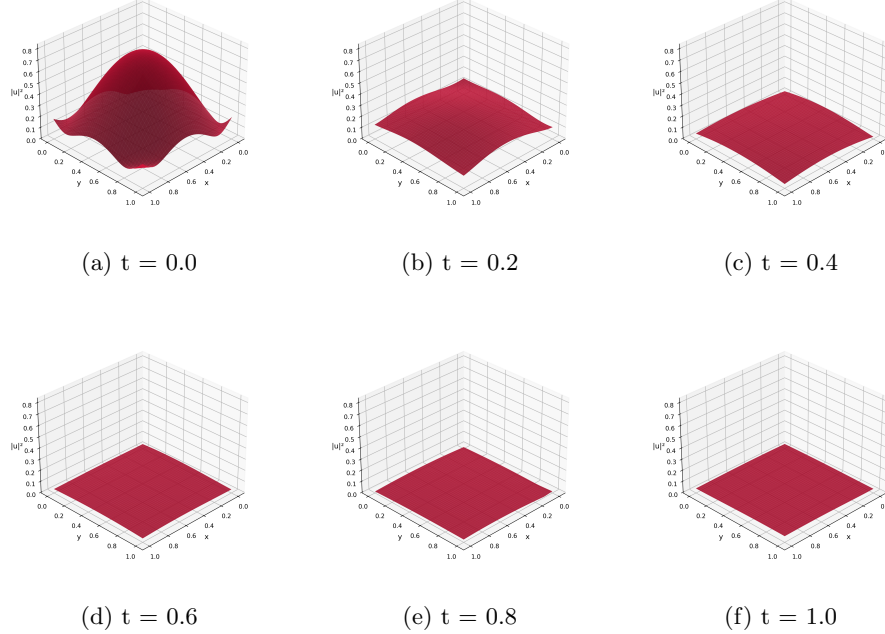


Figure 7: Time evolution of the solution of the free Schrödinger equation, obtained with the PINN.

where $V_0(x)$ is a time-independent potential and $V'(x, t)$ is a time-dependent potential.

As discussed in the introduction, the time-independent potential can be approximated by combinations of harmonic and double well potentials that describe the energy profile of certain internal coordinates of a molecule. Here, we therefore choose

$$V_0(x) = \underbrace{ax_1^2}_{V_{\text{harmonic}}} + \underbrace{bx_2^4 - cx_2^2}_{V_{\text{double well}}} + dx_1x_2,$$

where a, b, c and d are constants. The time-independent potential is shown in Figure 2 a).

For the time-dependent potential, we draw inspiration from photophysics, where time-dependent behavior is often introduced by interaction of electrons with light. In the simplest case, this interaction is described by the dipole approximation:

$$V'(x, t) = -\vec{E}(t) \cdot \vec{x},$$

where $\vec{E}(t) = (E_1(t), E_2(t))$ is the electric field of the light and $\vec{x} = (x_1, x_2)$ is the position of the electron.

To model the time-dependent potential, we will use a laser pulse with a Gaussian temporal envelope and uniform spatial profile:

$$\vec{E}(t) = E_0 \cdot \exp\left(-\frac{(t - t_c)^2}{2\sigma^2}\right) \cdot \cos(2\pi\omega t + \phi) \cdot \vec{e}_i,$$

where E_0 is the peak amplitude, t_c is the center time, σ is the temporal width (related to the full width at half maximum by $\sigma = \text{FWHM}/(2\sqrt{2\ln(2)})$), ω is the angular frequency, ϕ is the phase, and \vec{e}_i is the polarization vector in space. A simplified profile of a laser pulse in time is shown in Figure 8.

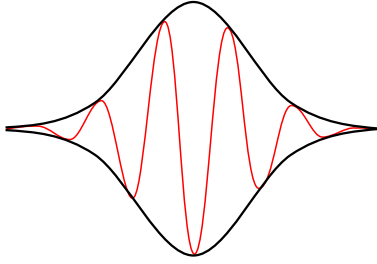


Figure 8: Schematic illustration of a laser pulse with Gaussian temporal envelope (black curve) and oscillating electric field (red curve). The envelope is characterized by amplitude E_0 , center time t_c , and width σ , while the oscillation has frequency ω and phase ϕ .

The time evolution of the resulting potential is shown in Figure 9.

Initial condition

For this potential, there is of course no analytical solution of the time-dependent Schrödinger equation to compare the results with. Therefore, we use the solution of the time-independent Schrödinger equation as initial condition.

$$\begin{aligned} -\Delta u(x) + V(x)u(x) &= Eu(x), \quad x \in \Omega, \\ u(x) &= 0, \quad x \in \partial\Omega. \end{aligned}$$

Following the same procedure as in the previous section, the variational formulation is given by

$$\int_{\Omega} \nabla u \cdot \nabla v dx + \int_{\Omega} V(x)uv dx = E \int_{\Omega} uv dx, \quad \forall v \in V,$$

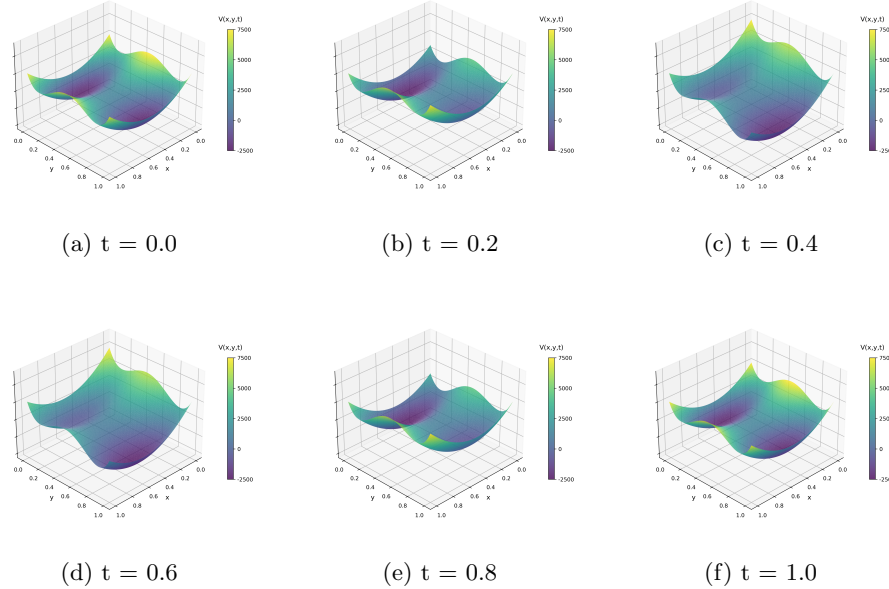


Figure 9: Time evolution of the time-dependent model potential, which is a combination of a harmonic and a double well potential, and the interaction with a laser pulse.

which we solve with the FEM, using the same parameters as in the previous section. Here, we take the solution with smallest eigenvalue E , which is the energetic ground state of the system, and which is shown in Figure 10. As we can see, the solution is localized in one of the two wells of potential.

FEM Solution

We solve the time-dependent Schrödinger equation with the time-dependent model potential, using the following parameters:

- Meshing: Triangular mesh with 64×64 elements
 - Elements: P1 Lagrange elements
 - Time step size: $\Delta t = 0.000001$

The evolution of the solution for different time steps is shown in Figure 11.

While for the free Schrödinger equation, the squared absolute value of the wave function is constant over time, we see that it now evolves in time, which is due

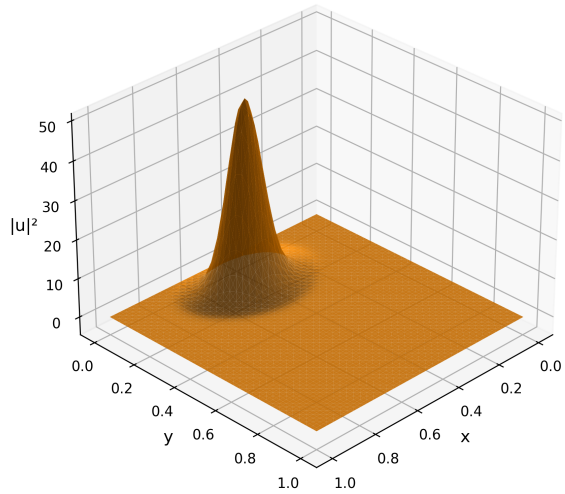


Figure 10: Initial condition as the ground state solution of the time-independent Schrödinger equation with the model potential.

to the time-dependent potential. Furthermore, we see that the wave function is not localized in one of the two wells of potential anymore, but rather spreads over the whole domain. From a physical point of view, this is enabled by the laser pulse, which effectively lowers the potential barrier between the two wells of potential over time. Very interestingly, the wave function shows interference patterns, a phenomenon exclusively observed in quantum mechanics.

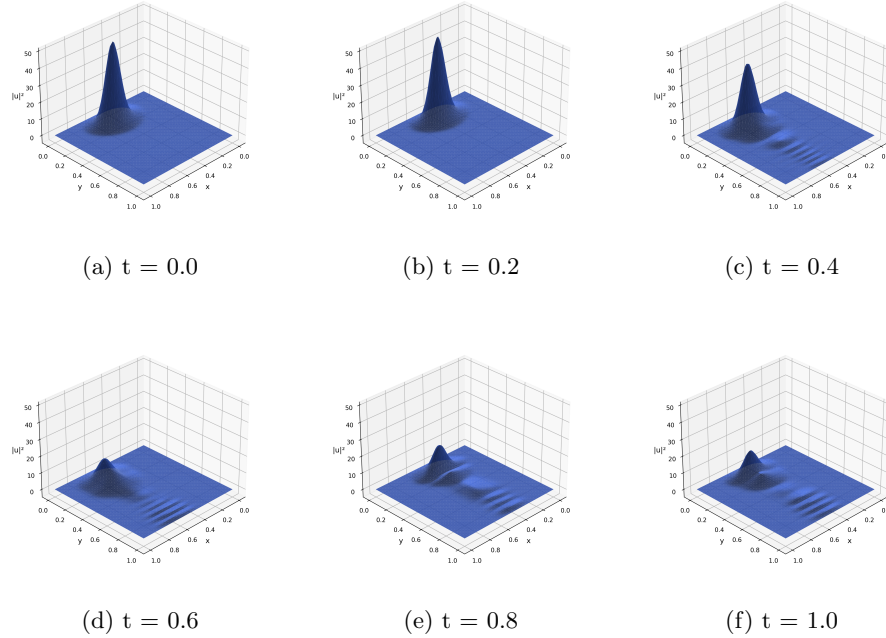


Figure 11: Time evolution of the solution of the Schrödinger equation with the time-dependent model potential, obtained with the FEM.

5 Outlook

In both FEM scenarios—free evolution and time-dependent potential—we observe that the norm of the wave function is not conserved over time. This is a direct consequence of the Backward Euler scheme, which lacks norm preservation and introduces a significant dependence on the time step size. To address this limitation, future work could explore norm-conserving time integrators such as the Crank–Nicolson method, higher-order schemes, or the use of periodic boundary conditions to mitigate boundary artifacts.

For PINNs, the primary challenge lies in the instability of the solution, which tends to collapse toward the trivial zero function. Improving stability will require more robust regularization strategies—particularly to enforce norm conservation more effectively—or the development of alternative loss formulations that better capture the underlying physics.